PHYSICAL REVIEW D **82,** 076006 (2010)

Scalar resonance effects on the B_s-$\bar{B}_s$ mixing angle

O. Leitner,* J.-P. Dedonder,† and B. Loiseau‡

Laboratoire de Physique Nucléaire et de Hautes Énergies, Groupe Théorie, Université Pierre et Marie Curie et Université Paris-Diderot, IN2P3 and CNRS, 4 place Jussieu, 75252 Paris, France

B. El-Bennich§

Physics Division, Argonne National Laboratory, Argonne, Illinois 60439, USA‖

(Received 30 March 2010; revised manuscript received 4 August 2010; published 21 October 2010)

The $B_s^0 \to J/\psi\phi$ and $B_s^0 \to J/\psi f_0(980)$ decays are analyzed within generalized QCD factorization including all leading-order corrections in α_s: We point out that the ratio of our calculated widths, $\Gamma(B_s^0 \to J/\psi f_0(980), f_0(980) \to \pi^+\pi^-)/\Gamma(B_s^0 \to J/\psi\phi, \phi \to K^+K^-)$, strongly indicates that S-wave effects in the $f_0(980)$'s daughter pions or kaons cannot be ignored in the extraction of the $B_s - \bar{B}_s$ mixing angle, $-2\beta_s$, from the $B_s^0 \to \phi J/\psi$ decay amplitudes.

DOI: 10.1103/PhysRevD.82.076006 PACS numbers: 11.30.Er, 13.25.Hw, 13.30.Eg

I. INTRODUCTION

In the standard model, CP violation is predicted in weak decays thanks to the single phase of the Cabibbo-Kobayashi-Maskawa matrix. It is also well known that such a weak phase is not sufficient to generate a CP violating decay amplitude. Strong phases are necessary and their strength may significantly enhance the effect of the weak phase. Therefore, hadronic effects, such as resonances of daughter particles in S and higher waves, require a careful analysis in the determination of CP violating phases in hadronic two- and three-body decays [1–4].

The antimatter-matter asymmetry is expected to be very small in weak decays of B_s mesons; any observed deviation may well be a signal of physics whose origins lie beyond the standard model. In the $B_s^0 \to J/\psi\phi$ channel, recent measurements by the CDF [5] and DØ [6,7] Collaborations of the $B_s - \bar{B}_s$ mixing phase, $-2\beta_s$, while not definitive, are considerably larger than standard model predictions. Taking advantage of the fact that the $B_s^0 \to J/\psi f_0(980)$ channel does not require any angular analysis, one can compute the ratio between the $B_s^0 \to J/\psi\phi$ and $B_s^0 \to J/\psi f_0(980)$ decay widths in order to estimate the $\pi^+\pi^-$ S-wave effect on the value of β_s. A first qualitative attempt to predict the ratio,

$$\mathcal{R}_{f_0/\phi} = \frac{\Gamma(B_s^0 \to J/\psi f_0(980), f_0(980) \to \pi^+\pi^-)}{\Gamma(B_s^0 \to J/\psi\phi, \phi \to K^+K^-)}, \quad (1)$$

was made by Stone and Zhang [8] and gives a result of the order of 20%–30%. Their estimate relies on experimental data on $D_s^+ \to f_0(980)\pi^+$ and $D_s^+ \to \phi\pi^+$ decays and seems to indicate that the S-wave contribution of $f_0(980) \to K^+K^-$ cannot be ignored when analyzing the angle β_s in $B_s^0 \to J/\psi\phi$. Likewise, Xie *et al.* found the effect of an S-wave component on $2\beta_s$ to be of the order of 10% in the ϕ resonance region [9].

Based on the QCD factorization (QCDF) formalism, we perform a first robust calculation of the ratio $\mathcal{R}_{f_0/\phi}$. To this end, all the available observables (polarizations and branching ratio in $B_s^0 \to J/\psi\phi$) are used to effectively constrain the analysis of the $B_s^0 \to J/\psi\phi$ channel. The branching ratio and CP asymmetry are then predicted for $B_s^0 \to J/\psi f_0(980)$, where we assume that merely the $s\bar{s}$ component of the $f_0(980)$ is involved in the hadronic $B_s \to f_0(980)$ transition matrix element.

In Sec. II we introduce the general expressions for the $B_s^0 \to J/\psi\phi$ and $B_s^0 \to J/\psi f_0(980)$ weak decay amplitudes; whereas, Secs. III and IV provide the details on the leading-order corrections in α_s for both these amplitudes, respectively. In Sec. V, we list all numerical values of input parameters and briefly recall our model for the $B_s \to f_0(980)$ transition form factor [10] on which the ratio $\mathcal{R}_{f_0/\phi}$ directly depends; we also define the parametrization for the $B_s \to \phi$ form factor. Section VI is devoted to our results, and finally, conclusions are drawn in Sec. VII.

II. GENERAL FORM OF THE $B_s^0 \to \phi J/\psi$ AND $B_s^0 \to f_0(980)J/\psi$ DECAY AMPLITUDES

It is important to realize beforehand that the application of QCDF, following Refs. [11–14], to B_s^0 decays into a heavy-light final state is not self-evident. In both final states, $\phi J/\psi$ and $f_0(980)J/\psi$, the s-spectator quark is absorbed by the light meson while the emitted meson is heavy, in which case QCDF is not reliable [11]. Nonetheless, as argued in Refs. [15,16] and more recently in Ref. [17], the production of a heavy charmonium $\bar{q}q$ pair bears "color transparency" properties similar to those of a light meson, provided this color-singlet pair is small compared to the inverse strong interaction scale, $1/\Lambda_{\rm QCD}$. This

*leitner@lpnhe.in2p3.fr
†dedonder@univ-paris-diderot.fr
‡loiseau@lpnhe.in2p3.fr
§bennich@anl.gov
‖Present address: LFTC, Universidade Cruzeiro do Sul, Rua Galvão Bueno, 868, São Paulo, 01506-000 SP, Brazil.

was explicitly demonstrated in next-to-leading order calculations for exclusive B decays to J/ψ final states ($J/\psi K, J/\psi K^*$), where infrared divergences were shown to cancel [15,16].

In the following, we present the B_s^0 decay amplitudes in which the short- and long-distance contributions are factorized in the approximation of a quasi two-body state, M_1M_2, where either $M_1M_2 = f_0(980)J/\psi$ or $M_1M_2 = \phi J/\psi$. We begin with the $B_s^0 \to \phi J/\psi$ amplitude which can be written for each helicity, $h = -1, 0, 1$, as [14]

$$\begin{aligned}\mathcal{A}^{\,h}_{B_s^0\to\phi J/\psi} = \sum_{q=u,c} \lambda_q \{A^h_{\phi J/\psi}[\delta_{qc}(a_2^{q,h}(m_b) + \zeta^h) \\ + a_3^{q,h}(m_b) + a_5^{q,h}(m_b) + a_7^{q,h}(m_b) \\ + a_9^{q,h}(m_b)]\}_{\phi J/\psi}. \end{aligned} \tag{2}$$

Summing over all the possible helicities, the squared modulus of the total amplitude reads

$$\begin{aligned}|\mathcal{A}_{B_s^0\to\phi J/\psi}|^2 = |\mathcal{A}^{h=-1}_{B_s^0\to\phi J/\psi}|^2 + |\mathcal{A}^{h=0}_{B_s^0\to\phi J/\psi}|^2 \\ + |\mathcal{A}^{h=+1}_{B_s^0\to\phi J/\psi}|^2. \end{aligned} \tag{3}$$

The $\bar{B}_s^0 \to \phi J/\psi$ decay amplitude is obtained by exchange of helicity signs, $h = +1 \to h = -1$, and replacing λ_q by its complex conjugate. The $B_s^0 \to f_0(980)J/\psi$ amplitude is

$$\begin{aligned}\mathcal{A}_{B_s^0\to f_0 J/\psi} = \sum_{q=u,c} \lambda_q \{A_{f_0 J/\psi}[\delta_{qc}(a_2^q(m_b) + \zeta) + a_3^q(m_b) \\ + a_5^q(m_b) + a_7^q(m_b) + a_9^q(m_b)]\}_{f_0 J/\psi}. \end{aligned} \tag{4}$$

The different elements entering in the amplitudes (2) and (4) are defined in Eqs. (6), (7), (15), (22), and (24). The CP conjugate $\bar{B}_s^0$ decay amplitude is again found by replacing λ_q by its complex conjugate.

With the generic amplitude, $\mathcal{A}_{B_s^0\to M_1 J/\psi}$, the branching ratio,

$$\begin{aligned}\mathcal{B}(B_s^0 \to M_1 J/\psi) \\ = \frac{1}{\Gamma_{B_s^0}} \frac{1}{16\pi m_{B_s^0}^3} \lambda^{1/2}(1, m_{M_1}^2/m_{B_s^0}^2, m_{J/\psi}^2/m_{B_s^0}^2)|A_{B_s^0\to M_1 J/\psi}|^2, \end{aligned} \tag{5}$$

can be computed. The J/ψ mass is noted $m_{J/\psi}$, while $m_{M_1} = m_{f_0(980)}$ or m_ϕ denote the $f_0(980)$ and ϕ masses; the triangle function is $\lambda(x, y, z) = (x + y - z)^2 - 4xy$. In Eq. (5), $\Gamma_{B_s^0} = 1/\tau_{B_s^0}$ is the B_s^0 decay width with $\tau_{B_s^0} = (1.470 \pm 0.026)$ ps [18] and $m_{B_s^0}$ is the B_s^0 mass. For the Cabibbo-Kobayashi-Maskawa elements in Eqs. (2) and (4), we use the Wolfenstein parametrization,

$$\begin{aligned}\lambda_u = V_{ub}^\star V_{us} = A\lambda^4(\rho + i\eta), \\ \lambda_c = V_{cb}^\star V_{cs} = A\lambda^2\left(1 - \frac{\lambda^2}{2}\right), \end{aligned} \tag{6}$$

with the Wolfenstein parameters $A = 0.814$, $\rho = 0.1385$, $\eta = 0.358$, and $\lambda = 0.2257$ [18].

A. Nonperturbative amplitude

1. The case of the scalar-vector decay

The scalar-vector factor, $A_{f_0 J/\psi}$, in Eq. (4) is given by

$$\begin{aligned}A_{f_0 J/\psi} = \langle f_0(p_{f_0})|\bar{b}\gamma\mu(1 - \gamma 5)s|B_s^0(p_{B_s^0})\rangle \\ \times \langle J/\psi(p_{J/\psi}, \varepsilon^*_{J/\psi})|\bar{c}\gamma^\mu c|0\rangle, \end{aligned} \tag{7}$$

where the hadronic matrix element which describes the transition between the B_s^0 and a scalar meson, f_0, with the respective four-momenta $p_{B_s^0}$ and p_{f_0} is [19]

$$\begin{aligned}\langle f_0(p_{f_0})|\bar{b}\gamma_\mu(1 - \gamma_5)s|B_s^0(p_{B_s^0})\rangle \\ = \left(p_{B_s^0} + p_{f_0} - \frac{m_{B_s^0}^2 - m_{f_0}^2}{q^2} q\right)_\mu F_1^{B_s^0\to f_0}(q^2) \\ + \frac{m_{B_s^0}^2 - m_{f_0}^2}{q^2} q_\mu F_0^{B_s^0\to f_0}(q^2), \end{aligned} \tag{8}$$

with $q = p_{B_s^0} - p_{f_0}$, $q^2 = m_{J/\psi}^2$ and where $F_1^{B_s^0\to f_0}(q^2)$ and $F_0^{B_s^0\to f_0}(q^2)$ are the vector and scalar form factors, respectively. In Eq. (7), the leptonic decay constant, $f_{J/\psi}$, of the J/ψ vector meson, with four-momentum, $p_{J/\psi}$, and polarization, $\varepsilon^*_{J/\psi}$, is defined as

$$\langle J/\psi(p_{J/\psi}, \varepsilon^*_{J/\psi})|\bar{c}\gamma^\mu c|0\rangle = -if_{J/\psi} m_{J/\psi} \varepsilon^{\mu *}_{J/\psi}. \tag{9}$$

The scalar-vector factor, given by the product of Eqs. (8) and (9), is then obtained as

$$A_{f_0 J/\psi} = -i\frac{G_F}{\sqrt{2}} 2m_{J/\psi} \epsilon^*_{J/\psi} \cdot p_{B_s^0} F_1^{B_s^0\to f_0}(m_{J/\psi}^2) f_{J/\psi}, \tag{10}$$

with $4m_{J/\psi}^2|\epsilon^*_{J/\psi} \cdot p_{B_s^0}|^2 = m_{B_s^0}^2 \lambda^{1/2}(m_{B_s^0}^2, m_{J/\psi}^2, m_{f_0}^2)$ and the Fermi constant, $G_F = 1.16 \times 10^{-5}\text{GeV}^{-2}$. The $B_s^0 \to f_0$ transition form factor $F_1^{B_s^0\to f_0}(m_{J/\psi}^2)$ will be discussed in Sec. V.

2. The case of the vector-vector decay

For the case of two vector mesons, M_1 and M_2, the helicity formalism requires the introduction of three polarization four-vectors, $\epsilon_{M_j,k}$ ($j = 1, 2$ and $k = 1, 2, 3$) for each spin-1 particle, M_j,

$$\begin{aligned}\epsilon_{M_j,1} = (0, \vec{\epsilon}_{M_j,1}), \qquad \epsilon_{M_j,2} = (0, \vec{\epsilon}_{M_j,2}), \\ \epsilon_{M_j,3} = (|\vec{p}_{M_j}|/m_{M_j}, E_{M_j}\hat{p}_{M_j}/m_{M_j}), \end{aligned} \tag{11}$$

where m_{M_j}, p_{M_j} and E_{M_j} are the mass, the momentum and the energy of the vector meson, M_j, respectively. The energies E_{M_1}, E_{M_2} are given by

$$E_{M_{1,2}} = \frac{1}{2m_{M_{2,1}}}(m_{B_s^0}^2 - m_{M_1}^2 - m_{M_2}^2). \tag{12}$$

In Eq. (11), $\hat{p}_{M_j}$ is defined as the unit vector along the momentum: $\hat{p}_{M_j} = \vec{p}_{M_j}/|\vec{p}_{M_j}|$.

The three polarization four-vectors, $\epsilon_{M_j,k}$, also satisfy the following relations:

$$\epsilon_{M_j,k}{}^2 = -1, \quad \text{and} \quad \epsilon_{M_j,k}\cdot\epsilon_{M_j,l} = 0, \quad \text{for } k \neq l. \tag{13}$$

The vectors $\vec{\epsilon}_{M_j,1}$, $\vec{\epsilon}_{M_j,2}$, and $\vec{\epsilon}_{M_j,3}$ form an orthogonal basis in which $\vec{\epsilon}_{M_j,1}$ and $\vec{\epsilon}_{M_j,2}$ describe the transverse polarizations while $\vec{\epsilon}_{M_j,3}$ is the longitudinal polarization vector. With these three vectors, one builds up the helicity basis,

$$\begin{aligned}
\epsilon_{M_j,+} &= \frac{1}{\sqrt{2}}(\epsilon_{M_j,1} + i\epsilon_{M_j,2}) = \frac{1}{\sqrt{2}}(0,+1,i,0),\\
\epsilon_{M_j,-} &= \frac{1}{\sqrt{2}}(\epsilon_{M_j,1} - i\epsilon_{M_j,2}) = \frac{1}{\sqrt{2}}(0,-1,i,0),\\
\epsilon_{M_j,0} &= \epsilon_{M_j,3},
\end{aligned} \tag{14}$$

and $\epsilon_{M_1,\pm} = \epsilon_{M_2,\mp}$. In Eq. (14), the new four-vectors $\epsilon_{M_j,+}$, $\epsilon_{M_j,-}$, and $\epsilon_{M_j,0}$ are eigenvectors of the helicity operator corresponding to the eigenvalues $h = +1, -1$, and 0, respectively.

The vector-vector factor, $A^h_{M_1M_2}$, in Eq. (2) is

$$\begin{aligned}
A^h_{M_1M_2} &= \langle M_1(p_{M_1},\varepsilon^*_{M_1})|\bar{b}\gamma_\mu(1-\gamma_5)q|B_s^0(p_{B_s^0})\rangle\\
&\quad\times\langle M_2(p_{M_2},\varepsilon^*_{M_2})|\bar{q}\gamma^\mu q'|0\rangle,
\end{aligned} \tag{15}$$

where, in the B_s^0 rest-frame, the vector mesons M_1 and M_2 have opposite momentum $\vec{p}_{M_1} = -\vec{p}_{M_2}$ along the z direction and $\epsilon_{M_j,0}\cdot p_{M_j} = 0$.

The matrix hadronic element of a $P \to V$ transition can be decomposed into Lorentz invariants as [16,19,20]

$$\begin{aligned}
&\langle M_j(p_{M_j},\varepsilon^*_{M_j})|\bar{b}\gamma_\mu(1-\gamma_5)q|B_s^0(p_{B_s^0})\rangle\\
&\quad= \varepsilon^*_{M_j,\mu}(m_{B_s^0}+m_{M_j})A_1^{B_s^0\to M_j}(q^2)\\
&\quad- (p_{B_s^0}+p_{M_j})_\mu(\varepsilon^*_{M_j}\cdot p_{B_s^0})\frac{A_2^{B_s^0\to M_j}(q^2)}{m_{B_s^0}+m_{M_j}}\\
&\quad- q_\mu(\varepsilon^*_{M_j}\cdot p_{B_s^0})\frac{2m_{M_j}}{q^2}[A_3^{B_s^0\to M_j}(q^2) - A_0^{B_s^0\to M_j}(q^2)]\\
&\quad+ i\epsilon_{\mu\nu\alpha\beta}\varepsilon^{*\nu}_{M_j}p^\alpha_{B_s^0}p^\beta_{M_j}\frac{2V^{B_s^0\to M_j}(q^2)}{m_{B_s^0}+m_{M_j}},
\end{aligned} \tag{16}$$

where the form factors $A_0^{B_s^0\to M_j}(q^2)$, $A_1^{B_s^0\to M_j}(q^2)$, $A_2^{B_s^0\to M_j}(q^2)$, and $A_3^{B_s^0\to M_j}(q^2)$ obey the following exact relations:

$$A_3^{B_s^0\to M_j}(q^2) = \frac{m_{B_s^0}+m_{M_j}}{2m_{M_j}}A_1^{B_s^0\to M_j}(q^2) - \frac{m_{B_s^0}-m_{M_j}}{2m_{M_j}}A_2^{B_s^0\to M_j}(q^2), \tag{17}$$

as well as for $q^2 = 0$, $A_3^{B_s^0\to M_j}(0) = A_0^{B_s^0\to M_j}(0)$.

Specifically for $M_1 = \phi$, and $M_2 = J/\psi$, the helicity dependent vector-vector factor $A^h_{\phi J/\psi}$ in Eq. (2) has thus the following form:

$$\begin{aligned}
A^{(h=0)}_{\phi J/\psi} &= i\frac{G_F}{\sqrt{2}}f_{J/\psi}[-m_\phi(m_{B_s^0}+m_\phi)A_1^{B_s^0\to\phi}(m^2_{J/\psi})\\
&\quad+(m^2_{B_s^0}+m^2_\phi-m^2_{J/\psi})A_0^{B_s^0\to\phi}(m^2_{J/\psi})];
\end{aligned} \tag{18a}$$

$$A^{(h=\pm1)}_{\phi J/\psi} = i\frac{G_F}{\sqrt{2}}m_{B_s^0}m_{J/\psi}f_{J/\psi}F_\mp^{B_s^0\to\phi}(m^2_{J/\psi}). \tag{18b}$$

In Eq. (18b), the transition form factors $F_\pm^{B_s^0\to\phi}(q^2 = m^2_{J/\psi})$ are

$$F_\pm^{B_s^0\to\phi}(m^2_{J/\psi}) = \left(1+\frac{m_\phi}{m_{B_s^0}}\right)A_1^{B_s^0\to\phi}(m^2_{J/\psi}) \mp \frac{2|\vec{p}_{B_s^0}|}{m_{B_s^0}+m_\phi}V^{B_s^0\to\phi}(m^2_{J/\psi}), \tag{19}$$

where the center-of-mass momentum $|\vec{p}_{B_s^0}|$ is defined as

$$|\vec{p}_{B_s^0}| = \frac{\sqrt{(m^2_{B_s^0}-M_+^2)(m^2_{B_s^0}-M_-^2)}}{2m_{B_s^0}}, \tag{20}$$

with $M_\pm = m_{J/\psi} \pm m_\phi$. We note that a somewhat different form for $A^{(h=0)}_{\phi J/\psi}$ was derived in Ref. [20], which seems to approximate the vector mesons as light mesons. The form factors $A_0^{B_s^0\to\phi}(m^2_{J/\psi})$ and $A_1^{B_s^0\to\phi}(m^2_{J/\psi})$ in Eqs. (18a) and (19), as well as $V^{B_s^0\to\phi}(m^2_{J/\psi})$ in Eq. (19) are defined in Sec. V. Reference [14] asserts that when neglecting vector meson masses, Eq. (18a) reduces to

$$A^{(h=0)}_{\phi J/\psi} = i\frac{G_F}{\sqrt{2}}f_{J/\psi}m^2_{B_s^0}A_0^{B_s^0\to\phi}(m^2_{J/\psi}). \tag{21}$$

The numerical effects in the calculated values of $B_s^0 \to J/\psi\phi$ and $B_s^0 \to J/\psi f_0(980)$ branching ratios are too important to justify such an approximation.

B. Perturbative amplitude

The $a_n^{q,h}(\mu)$ coefficients that appear in Eqs. (2) and (4) are linear combinations of Wilson coefficients, $C_n(\mu)$, either at the scale $\mu = m_b$ or $m_b/2$ (see below):

$$a_n^{q,h}(m_b) = \left[C_n(m_b) + \frac{C_{n\pm1}(m_b)}{N_c}\right]N_n(J/\psi) + P_n^{q,h}(J/\psi) + \frac{C_{n\pm1}(m_b)}{N_c}\frac{C_F}{4\pi}\alpha_s(m_b)V_n^h(J/\psi) + \pi C_F\alpha_s(m_b/2)\frac{C_{n\pm1}(m_b/2)}{N_c^2}H_n^h(M_1J/\psi). \quad (22)$$

The superscript (h) refers to the helicity dependence of $a_n^{q,h}(\mu)$ in the case where B_s^0 decays into two vector mesons. This superscript is dropped in the scalar-vector case. There is no flavor dependence in $a_n^{q,h}(\mu)$ for $n = 1, 2$. In Eq. (22), the upper (lower) signs in $C_{n\pm1}(\mu)$ apply when n is odd (even) and

$$N_n(J/\psi) = 0, \qquad n \in \{6, 8\}, \quad \text{else } N_n(J/\psi) = 1. \quad (23)$$

The Wilson coefficients, $C_n(\mu)$, in the naive dimensional regularization scheme are taken at the hard scale m_b for the vertex, $V_n^h(J/\psi)$, and penguin, $P_n^{q,h}(J/\psi)$, corrections; whereas, in the hard scattering, $H_n^h(M_1J/\psi)$, amplitudes they are evaluated at $m_b/2$ since those contributions involve the spectator quark. The strong coupling constants at these scales are $\alpha_s(m_b) = 0.224$ and $\alpha_s(m_b/2) = 0.286$ [18], while the number of active flavors is $n_F = 5$, the color number $N_c = 3$ and $C_F = (N_c^2 - 1)/2N_c$.

C. Suppressed higher order corrections and possibility of new physics

There are no contributions, such as given by the annihilation operators derived in Ref. [13], to the two decays considered here. This is because for the final states, $J/\psi\phi$ and $J/\psi f_0(980)$, both mesons are simultaneously flavor *and* color singlets. At tree level, for instance, the $W^\pm$ exchange diagram produces the charmonium $\bar{c}c$, yet the creation of the $\bar{s}s$ which hadronizes to an $f_0(980)$ or ϕ must proceed via multiple gluons or by means of photon/Z exchange. The annihilation is thus either strongly (Zweig) suppressed in α_s or the suppression is in the electromagnetic coupling constant $\alpha_{\rm em}$.

On the other hand, as will be discussed in Sec. VI, if we account for vertex, penguin and hard-scattering corrections only, the $B_s^0 \to J/\psi\phi$ observables are only moderately well reproduced. As can be seen in Table IX, the branching ratio, for instance, is about 20% too large (although still within the experimental errors). We therefore allow for additional phenomenological amplitudes that mock up ''other'' contributions, be it from annihilation topologies expected to be strongly suppressed or possible physics beyond the standard model [21]. These are included in Eqs. (2) and (4) with the amplitudes, ζ^h and ζ, conveniently scaled as

$$\zeta^{(h)} = \frac{B_{M_1J/\psi}}{A^{(h)}_{M_1J/\psi}}X_C. \quad (24)$$

The factor $B_{M_1J/\psi}$ is chosen to be a product of decay constants, either

$$B_{f_0J/\psi} = -i\frac{G_F}{\sqrt{2}}f_{B_s^0}\bar{f}_{f_0}f_{J/\psi}, \quad (25)$$

if $M_1 = f_0(980)$ or

$$B_{\phi J/\psi} = i\frac{G_F}{\sqrt{2}}f_{B_s^0}f_\phi f_{J/\psi}, \quad (26)$$

if $M_1 = \phi$, while the factor X_C is a complex parameter discussed in Sec. V C. We note that the decay constant, f_{f_0}, vanishes due to charge conjugation invariance, wherefore the scalar light cone distributions amplitude (LCDA) is normalized to $\bar{f}_{f_0} = f_{f_0}m_{f_0}/(m_{u,d}(\mu) - m_{u,d}(\mu))$, which is finite [22]. We shall return to this issue in Sec. IV.

D. The ratio $\mathcal{R}_{f_0/\phi}$

Prior to discussing the various $\alpha_s(\mu)$ corrections to the amplitudes, $a_n^{p,h}(\mu)$, it may be of interest to observe the qualitative behavior of the ratio, $\mathcal{R}_{f_0/\phi}$, in terms of the scales $\Lambda_{\rm QCD}$ and m_b. A naive factorization analysis yields a hierarchy of helicity amplitudes for B into vector-vector decays [14],

$$\mathcal{A}^{(h=0)}_{B_s^0\to\phi J/\psi} : \mathcal{A}^{(h=+1)}_{B_s^0\to\phi J/\psi} : \mathcal{A}^{(h=-1)}_{B_s^0\to\phi J/\psi} \Longleftrightarrow 1 : \frac{\Lambda_{\rm QCD}}{m_b} : \left(\frac{\Lambda_{\rm QCD}}{m_b}\right)^2, \quad (27)$$

while for $\bar{B}_s$ mesons the signs are exchanged ($h = +1 \to h = -1$). Furthermore, the amplitudes $\mathcal{A}^{(h=0)}_{B_s^0\to\phi J/\psi}$ and $\mathcal{A}_{B_s^0\to f_0J/\psi}$ are of same order in $\Lambda_{\rm QCD}/m_b$. With this estimation, the ratio $\mathcal{R}_{f_0/\phi}$ we are interested in becomes

$$\mathcal{R}_{f_0/\phi} = \frac{|\mathcal{A}_{B_s^0\to f_0J/\psi}|^2}{|\mathcal{A}^{(h=0)}_{B_s^0\to\phi J/\psi}|^2 + |\mathcal{A}^{(h=-1)}_{B_s^0\to\phi J/\psi}|^2 + |\mathcal{A}^{(h=+1)}_{B_s^0\to\phi J/\psi}|^2} \simeq \mathcal{O}(1) + \mathcal{O}\left(\frac{\Lambda_{\rm QCD}}{m_b}\right)^2 + \mathcal{O}\left(\frac{\Lambda_{\rm QCD}}{m_b}\right)^4. \quad (28)$$

Hence, $R_{f_0/\phi}$ is $\mathcal{O}(1)$ for $\Lambda_{\rm QCD}/m_b$ corrections.

Nonetheless, nonperturbative hadronic effects can spoil the naive factorization and violate the hierarchy in Eq. (27) ; so do electromagnetic penguin contributions where a photon with small virtuality subsequently converts into a vector meson [23].

III. QCDF CORRECTIONS FOR $B_s^0 \to \phi J/\psi$ DECAY AMPLITUDES

Because of the structure of the four-quark operators in heavy quark effective theory and the conservation of the flavor quantum numbers, the final state $M_1M_2 = \phi J/\psi$ is

created from the transition $B_s^0 \to \phi$ and the production of J/ψ from vacuum. As discussed in Sec. II, the decay amplitudes at leading order in $\Lambda_{\rm QCD}/m_b$ and $\alpha_s(m_b)$ are given by the factorized product of a transition form factor and a decay constant. Following Ref. [14], we only give QCD corrections that explicitly appear in the amplitude $\mathcal{A}^h_{B_s^0\to\phi J/\psi}$ of Eq. (2).

We discard terms proportional to $r = (m_{J/\psi}/m_{B_s})^2 \simeq 1/3$ in vertex corrections which stem from the presence of the charm quark in the loop diagram; we have numerically checked that their contributions to the $a_n^{q,h}(\mu)$ coefficients are negligible, all the more so when seen in the light of the large hadronic uncertainties of the form factors [see Secs. V A and V B]. We note that in the limit $r \to 0$, one recovers the vertex correction known from, for example, $B \to \pi\pi$ which is of course infrared safe.

Since the coefficients in the Gegenbauer expansion of the LCDA are poorly known for the scalar mesons, and only with non-negligible errors for the vector mesons $V = \phi$ and $V = J/\psi$, we limit ourselves to leading terms in the expansion. The leading twist-2 distribution and twist-3 two-particle distribution amplitudes are approximated by

$$\phi_V(x) = 6x(1-x) \tag{29}$$

and

$$\varphi_V(x) = 3(2x-1), \tag{30}$$

respectively. In the annihilation and hard-scattering amplitudes, the chiral coefficient, $r_\chi^V(\mu)$, is defined as

$$r_\chi^V(\mu) = \frac{2m_V}{m_b(\mu)}\frac{f_V^\perp(\mu)}{f_V} \simeq \frac{2m_V}{m_b(\mu)}, \tag{31}$$

where $f_V^\perp(\mu)$ is the transverse decay constant for any vector V and $\mu = m_b/2$.

A. Penguin contributions

The penguin contributions to the amplitude in Eq. (2) stems from the positive helicity, $h = +1$, amplitudes $P_{7,9}^{q,h=+1}(J/\psi)$ given in Ref. [14],

$$P_{7,9}^{q,h=+1}(J/\psi) = -\frac{\alpha_e}{3\pi}C_{7\gamma}^{\rm eff}(\mu)\frac{m_{B_s^0}m_b}{m_{J/\psi}^2} + \frac{2\alpha_e}{27\pi}(C_1(\mu) + N_cC_2(\mu))\left[\delta_{qc}\,\ln\frac{m_c^2}{\mu^2} + \delta_{qu}\,\ln\frac{\nu^2}{\mu^2} + 1\right], \tag{32}$$

whereas $P_{7,9}^{q,h=-1}(J/\psi) = 0$. In Eq. (32), $\mu = m_b$, $C_{7\gamma}^{\rm eff}(\mu) = C_{7\gamma}(\mu) - C_5(\mu)/3 - C_6(\mu)$, $\alpha_e = 1/129$ is the electromagnetic coupling constant and the scale ν refers to the $f_{J/\psi}$ decay constant scale. One also has $P_{3,5}^{q,h=\pm1}(J/\psi) = 0$ as well as $P_{3,5,7,9}^{q,(h=0)}(J/\psi) = 0$.

B. Vertex contributions

In $B_s^0 \to \phi J/\psi$, the electroweak vertex receives $\alpha_s(\mu)$ corrections to all $a_n^{q,h}(\mu)$ in the amplitudes $\mathcal{A}^h_{B_s^0\to\phi J/\psi}$. For $h = 0$, these are, with $\mu = m_b$,

$$V_n^{h=0}(J/\psi) = \begin{cases} 12\,\ln\left(\frac{m_b}{\mu}\right) - 3i\pi - \frac{27}{2}, \\ \quad \text{for } n \in \{2,3,9\}, \\ -12\,\ln\left(\frac{m_b}{\mu}\right) + 3i\pi + \frac{13}{2}, \\ \quad \text{for } n \in \{5,7\}; \end{cases} \tag{33}$$

whereas for $h = -1$, one has

$$V_n^{h=-1}(J/\psi) = \begin{cases} 12\,\ln\left(\frac{m_b}{\mu}\right) + \pi^2 - \frac{143}{4}, \\ \quad \text{for } n \in \{2,3,9\}, \\ -12\,\ln\left(\frac{m_b}{\mu}\right) - \pi^2 + \frac{95}{4}, \\ \quad \text{for } n \in \{5,7\}, \end{cases} \tag{34}$$

and for $h = +1$, one has

$$V_n^{h=+1}(J/\psi) = \begin{cases} 12\,\ln\left(\frac{m_b}{\mu}\right) + \frac{\pi^2}{2} - 6i\pi - \frac{71}{4}, \\ \quad \text{for } n \in \{2,3,9\}, \\ -12\,\ln\left(\frac{m_b}{\mu}\right) - \frac{\pi^2}{2} + 6i\pi + \frac{23}{4}, \\ \quad \text{for } n \in \{5,7\}. \end{cases} \tag{35}$$

C. Hard-scattering contributions

The gluon exchange between a J/ψ meson and the spectator s-quark leads to the hard-scattering amplitudes,

$$H_n^{h=0}(\phi J/\psi) = \pm 3\frac{B_{\phi J/\psi}}{A_{\phi J/\psi}^{h=0}}\frac{m_{B_s^0}}{\lambda_{B_s^0}}(r_\chi^\phi(\mu)X_H + 3), \tag{36}$$

for $h = 0$, $\mu = m_b/2$, and $\lambda_{B_s^0} = 0.350$ GeV [13]. The plus sign is for $n = 2, 3, 9$, and the minus sign for $n = 5, 7$. The phenomenological amplitude, X_H, parametrizes the end point divergence of the scalar meson's LCDA and is defined in Eq. (54). For the helicity, $h = +1$, the correction reads

$$H_n^{h=+1}(\phi J/\psi) = \mp 18\frac{B_{\phi J/\psi}}{A_{\phi J/\psi}^{h=+1}}\frac{f_\phi^\perp}{f_\phi}\frac{m_{J/\psi}}{\lambda_{B_s^0}}(X_H - 1), \tag{37}$$

where the minus sign applies to $n = 2, 3, 9$ and the plus sign to $n = 5, 7$. The helicity, $h = -1$, contribution is simply

$$H_n^{h=-1}(\phi J/\psi) = 0 \quad \text{for } n = 2,3,5,7,9. \tag{38}$$

IV. QCDF CORRECTIONS FOR $B_s^0 \to f_0(980)J/\psi$ DECAY AMPLITUDES

We now turn to the $B_s^0 \to J/\psi f_0(980)$ transition for which the $\alpha_s(\mu)$ corrections are all included following

Ref. [13] applied to an SV final state. For previously mentioned reasons, we solely employ the first nonvanishing leading term in the LCDA,

$$\phi_{f_0}(x) = 6x(1-x)[3B_1(\mu)(2x-1)], \tag{39}$$

where $B_1(m_b/2) = -0.54$ [22] is the $f_0(980)$'s first Gegenbauer moment and we remind that only odd moments contribute in case of charge-neutral scalar mesons. In particular, contrary to the pseudoscalar LCDA, the leading term $6x(1-x)B_0$ vanishes since $B_0 = (m_1(\mu) - m_2(\mu))/m_S$, where m_S is the scalar meson mass and $m_{1,2}(\mu)$ its running quark masses. The scalar twist-3 two-particle distribution is given by

$$\varphi_{f_0}(x) = 1. \tag{40}$$

The asymptotic forms of the LCDA, $\phi_{J/\psi}(x)$ [Eq. (29)] and $\varphi_{J/\psi}(x)$ [Eq. (30)], are used. As in the $B_s^0 \to \phi J/\psi$ decay, the J/ψ meson is created from vacuum whereas the transition $B_s^0 \to f_0(980)$ produces the scalar meson. Here, we only consider the $s\bar{s}$ component of the $f_0(980)$ since the flavor of the spectator quark in the tree and penguin topologies of B_s^0 decays is strange. There are no penguin corrections [13] to the $B_s^0 \to f_0(980)J/\psi$ decay amplitude in Eq. (4).

A. Vertex contributions

At the order of $\alpha_s(\mu)$, the vertex correction, $V_n(J/\psi)$, involves the leading twist distribution, $\phi_{J/\psi}(x)$, and a gluon kernel given in [13]. We derive from this the expressions

$$V_n(J/\psi) = \begin{cases} 12\ \ln\left(\frac{m_b}{\mu}\right) - 3i\pi - \frac{37}{2}, \\ \quad \text{for } n \in \{2, 3, 9\}, \\ -12\ \ln\left(\frac{m_b}{\mu}\right) + 3i\pi + \frac{13}{2}, \\ \quad \text{for } n \in \{5, 7\} \end{cases} \tag{41}$$

with $\mu = m_b$.

B. Hard-scattering contributions

The hard-scattering correction in case of an $f_0 J/\psi$ final state reads

$$H_n(f_0 J/\psi) = \pm 3 \frac{B_{f_0 J/\psi}}{A_{f_0 J/\psi}} \frac{m_{B_s^0}}{\lambda_{B_s^0}} (\bar{r}_\chi^{f_0}(\mu) X_H + 3B_1(\mu)), \tag{42}$$

where the plus sign applies to $n = 2, 3, 9$, the minus sign to $n = 5, 7$ and X_H is given, as in the case of the $\phi J/\psi$ final state, by Eq. (54).

The chiral coefficient, $\bar{r}_\chi^{f_0}(\mu)$, enters Eq. (42) rather than $r_\chi^{f_0}(\mu)$ defined as

$$r_\chi^{f_0}(\mu) = \frac{2m_{f_0}^2}{m_b(\mu)(m_1(\mu) - m_2(\mu))}. \tag{43}$$

The reason is that in case of neutral scalar mesons, $m_1(\mu) = m_2(\mu)$ and $r_\chi^{f_0}(\mu)$ diverges. On the other hand, it is known from C-conjugation invariance that the vector-decay constant of the neutral scalar meson must vanish. However, the quark equations of motions yield a relation between the scalar- and vector-decay constants, $\bar{f}_{f_0}$ and f_{f_0}, respectively:

$$\bar{f}_{f_0} = \frac{m_{f_0}}{m_1(\mu) - m_2(\mu)} f_{f_0}, \tag{44}$$

where $m_{f_0}\bar{f}_{f_0} = \langle 0|\bar{q}_2 q_1|f_0\rangle$. Since $\bar{f}_{f_0}$ is nonzero, the product $f_{f_0} m_{f_0}/(m_1(\mu) - m_2(\mu))$ is finite in the limit $m_1(\mu) \to m_2(\mu)$. We thus recombine, $f_{f_0} r_\chi^{f_0} = \bar{f}_{f_0} \bar{r}_\chi^{f_0}$, with

$$\bar{r}_\chi^{f_0}(\mu) = \frac{2m_{f_0}}{m_b(\mu)}. \tag{45}$$

V. NUMERICAL PARAMETERS

This section serves to summarize all parameter values required for numerical applications. The Wilson coefficients at the scales $\mu = m_b$ and $\mu = m_b/2$ used in this work are listed in Table I. For the meson masses, we refer to the latest PDG values [18], which are (in GeV):

$$m_{B_s^0} = 5.366, \quad m_{B_s^\star} = 5.412, \quad m_{f_0} = 0.980,$$
$$m_{J/\psi} = 3.096, \quad m_\phi = 1.019. \tag{46}$$

The running quark masses at $\mu = m_b = 4.2$ GeV are (in GeV),

$$m_b = 4.2, \quad m_c = 1.3,$$
$$m_s = 0.07, \quad m_{u,d} = 0.003, \tag{47}$$

and those at $\mu = m_b/2 = 2.1$ GeV are

$$m_b = 4.95, \quad m_c = 1.51,$$
$$m_s = 0.09, \quad m_{u,d} = 0.005. \tag{48}$$

We take the ϕ decay constant values from Ref. [14]: $f_\phi = (221 \pm 3)$ MeV and $f_\phi^\perp = (175 \pm 25)$ MeV. For the J/ψ meson, we use $f_{J/\psi} = (416 \pm 6)$ MeV [24] and $f_{J/\psi}^\perp = (405 \pm 5)$ MeV [16]. In the $B_s \to J/\psi f_0(980)$ channel, the $s\bar{s}$ component of the $f_0(980)$ is involved which implies the poorly known scalar decay constant $\bar{f}_{f_0}$: one theoretical estimate yields $\bar{f}_{f_0^s} = (180 \pm 15)$ MeV [25] whereas a much larger value $\bar{f}_{f_0^s}(1\text{ GeV}) = (370 \pm 20)$ MeV [$\bar{f}_{f_0^s}(2.1\text{ GeV}) = (460 \pm 25)$ MeV] is found in Ref. [22], both from coupling to the scalar $\bar{s}s$ current only (denoted by the superscript s in f_0^s, which we use henceforth). Similarly, several theoretical predictions exist for the leptonic B_s decay constants of which we select three values from unquenched lattice QCD: $f_{B_s^0} = (204 \pm 12^{+24}_{-23})$ MeV [26], $f_{B_s^0} = (259 \pm 32)$ MeV [27], and $f_{B_s^0} = (231 \pm 15)$ MeV [28].

TABLE I. Wilson coefficients at the $\mu = m_b$ and $\mu = m_b/2$ scales in the naive dimensional regularization scheme [12]. The coefficients $C_7(\mu) - C_{10}(\mu)$ must be multiplied by α_e.

	$C_1(\mu)$	$C_2(\mu)$	$C_3(\mu)$	$C_4(\mu)$	$C_5(\mu)$	$C_6(\mu)$	$C_7(\mu)$	$C_8(\mu)$	$C_9(\mu)$	$C_{10}(\mu)$	$C_{7\gamma}(\mu)$
$\mu = m_b$	1.081	−0.190	0.014	−0.036	0.009	−0.042	−0.011	0.06	−1.254	0.233	−0.318
$\mu = m_b/2$	1.137	−0.295	0.021	−0.051	0.010	−0.065	−0.24	0.096	−1.325	0.331	−0.364

To illustrate the sensitivity of the ratio $\mathcal{R}_{f_0/\phi}$ to the hadronic uncertainties, we exemplarily choose three different values for each decay constant: $f_{B_s^0} = 230$, 260, 290 MeV and $\bar{f}_{f_0^s} = 340$, 380, 420 MeV.

A. $B \to V$ transition form factor

Values for the $B_s^0 \to \phi$ transition form factors are taken from the pole-extrapolation model by Melikhov [19]:

$$A_0(q^2)^{B_s^0\to\phi} = \frac{a_0(0)}{(1 - \frac{q^2}{m^2_{B_s^0}})(1 - \sigma_1 \frac{q^2}{m^2_{B_s^0}} + \sigma_2 \frac{q^4}{m^4_{B_s^0}})}. \quad (49)$$

The form factor $V(q^2)^{B_s^0\to\phi}$ is given by a similar expression in which $a_0(0)$ is replaced by $v(0)$ and $m_{B_s^0}$ by $m_{B_s^\star}$ [19]. Next, the $A_1(q^2)^{B_s^0\to\phi}$ form factor is parametrized by

$$A_1(q^2)^{B_s^0\to\phi} = \frac{a_1(0)}{(1 - \sigma_1 \frac{q^2}{m^2_{B_s^\star}} + \sigma_2 \frac{q^4}{m^4_{B_s^\star}})}. \quad (50)$$

Finally, $A_2(q^2)^{B_s^0\to\phi}$ has the same functional form as $A_1(q^2)^{B_s^0\to\phi}$ where $a_1(0)$ is replaced by $a_2(0)$. In both, Eqs. (49) and (50), the momentum transfer is $q^2 = m^2_{J/\psi}$.

In Eqs. (49) and (50), the form factors at $q^2 = 0$ are $a_0(0) = 0.42$ ($v(0) = 0.44$) and $a_1(0) = 0.34$ ($a_2(0) = 0.31$). The extrapolation parameters are, for $A_0(q^2)^{B_s^0\to\phi}$, $\sigma_1 = 0.55$ and $\sigma_2 = 0.12$; for $V(q^2)^{B_s^0\to\phi}$, $\sigma_1 = 0.62$ and $\sigma_2 = 0.20$; for $A_1(q^2)^{B_s^0\to\phi}$, $\sigma_1 = 0.73$ and $\sigma_2 = 0.42$ and finally for $A_2(q^2)^{B_s^0\to\phi}$, $\sigma_1 = 1.30$ and $\sigma_2 = 0.52$. The respective values for the form factors at the value $q^2 = m^2_{J/\psi}$ are $A_0(q^2)^{B_s^0\to\phi} = 0.76$, $A_1(q^2)^{B_s^0\to\phi} = 0.42$, $A_2(q^2)^{B_s^0\to\phi} = 0.49$, and $V(q^2)^{B_s^0\to\phi} = 0.80$.

B. $B \to S$ transition form factor

We studied the transition form factor, $F_{0,1}^{B_s^0\to f_0^s}(q^2)$, in a comparative calculation using a dispersion relation and a covariant light front dynamics model [10]. To our knowledge, this form factor has only been calculated recently in QCD sum rules [29,30] and perturbative QCD [31] for $q^2 = 0$ and must be extrapolated to the value $F_{0,1}^{B_s^0\to f_0^s}(m^2_{J/\psi})$.

In our work [10], the transition form factors are derived from the constituent quark three-point function, the vertices of which are the weak interaction coupling, $\gamma_\mu(1 - \gamma_5)$, and two phenomenological Bethe-Salpeter amplitudes for the $B_{(s)}$ and $f_0(980)$ mesons. While the B_s can be parametrized with the leptonic decay constant (known from lattice-QCD simulations), the latter is more problematic since the $\bar{f}_{f_0^s}$ is poorly determined. In an attempt to formulate a suitable scalar $f_0(980)$ vertex function, we constrained its parameters by means of experimental quasi two-body branching fractions, $D_{(s)} \to f_0(980)P$, $P = \pi, K$. The advantage is that the $F_+^{B_s^0\to f_0^s}(q^2)$ and $F_-^{B_s^0\to f_0^s}(q^2)$ form factors,

$$\langle f_0^s(p_2)|\bar{s}\gamma_\mu(1 - \gamma_5)b|B_s^0(p_1)\rangle = F_+^{B_s^0\to f_0^s}(q^2)(p_1 + p_2)_\mu + F_-^{B_s^0\to f_0^s}(q^2)(p_1 - p_2)_\mu, \quad (51)$$

can be calculated for any physical timelike momentum transfer $q^2 = (p_1 - p_2)^2$. The superscript s is a reminder that the transition is to the $\bar{s}s$ component of the scalar meson and p_1 and p_2 are the B_s^0 and $f_0(980)$ four-momenta, respectively. We do stress that the $B_s \to f_0(980)$ form factor calculated by us in Ref. [10] does not assume a pure $\bar{s}s$ state of the $f_0(980)$. Instead, it was treated as a mixture of strange and nonstrange $\bar{q}q$ components related by a mixing angle which also yields the related form factor $F_{0,1}^{B\to f_0^{u,d}}(q^2)$. This angle was determined with experimental constraints [10] and the overall normalization of the transition form factor receives contributions from both states.

The form factors $F_\pm(q^2)$ (we suppress the flavor superscripts) are related to the set of vector and scalar form factors as

$$F_1(q^2) = F_+(q^2), \quad (52)$$

$$F_0(q^2) = F_+(q^2) + \frac{q^2}{m^2_{B_s^0} - m^2_{f_0}} F_-(q^2). \quad (53)$$

The form factor $F_1(q^2)$ we obtain in both the dispersion relation and covariant light front dynamics approaches agree at the maximum recoil point $q^2 = 0$. At large four-momentum transfer, specifically for $q^2 = m^2_{J/\psi} \simeq 10$ GeV^2, our model predictions differ significantly which is also known to occur for $B \to \pi$ transition form factors [32]. This is not surprising, as for large momentum transfers the final-state meson is less energetic and the soft physics of the bound states becomes more relevant. Since the models differ in their parametrization of the bound-state wave functions, it is clear that their inaccuracies are revealed in the form-factor predictions at large q^2.

In Ref. [30], we deduce from the author's extrapolation parametrization that $F_1^{B_s^0\to f_0^s}(m^2_{J/\psi}) \simeq 0.3$, which is compatible with our dispersion-relation prediction $\simeq 0.4$ within the errors. In Sec. VI, we will account for this rather large window of values and plot the ratio $\mathcal{R}_{f_0/\phi}$ as a function of $F_1^{B_s^0\to f_0^s}(m^2_{J/\psi})$.

C. Model parameters

The hard-scattering contributions involve end point divergences, which we choose to parametrize by

$$X_H = (1 + \rho_H \exp(i\phi_H)) \ln\frac{m_{B_s^0}}{\lambda_h}. \tag{54}$$

In case of a possible annihilation or other contribution, we simply write,

$$X_C = \rho_C \exp(i\phi_C) \tag{55}$$

which introduces four parameters, $0 < \rho_{C,H}$ and $0 < \phi_{C,H} < 360°$. We assume that $X_{C,H}^{h=0} = X_{C,H}^{h=-1} = X_{C,H}^{h=+1} = X_{C,H}$, as the vector ϕ and scalar $f_0(980)$ mesons have similar masses and we consider the $s\bar{s}$ component only. The hard-scattering corrections are expected to be of the order of $m_{B_s^0}/\lambda_h$ in Eq. (54), with $\lambda_h = 0.5$ GeV. The parameters $\rho_{C,H}$ and $\phi_{C,H}$ are chosen so as to reproduce the experimental data discussed in Sec. VI. We insert their values in the $B_s^0 \to J/\psi f_0$ decay amplitude (4) and then predict the branching ratio $\mathcal{B}(B_s^0 \to f_0 J/\psi)$.

VI. RESULTS AND EXPERIMENTAL DATA

In the $B_s^0 \to \phi J/\psi$ decay, one can define five observables: a longitudinal, parallel, and perpendicular polarization fraction, f_L,$f_\parallel$, and $f_\perp$, respectively,

$$f_k = \frac{|\mathcal{A}_k|^2}{|\mathcal{A}_L|^2 + |\mathcal{A}_\parallel|^2 + |\mathcal{A}_\perp|^2}, \qquad k = L, \parallel, \perp \tag{56}$$

as well as two relative phases, $\phi_\parallel$ and $\phi_\perp$,

$$\phi_k = \arg\left(\frac{\mathcal{A}_k}{\mathcal{A}_L}\right), \qquad k = \parallel, \perp, \tag{57}$$

where we have abbreviated, $L = \mathcal{A}^{(h=0)}_{s0\to\phi J/\psi}$, $\mathcal{A}\parallel = [\mathcal{A}^{(h=+1)}_{s0\to\phi J/\psi} + \mathcal{A}^{(h=-1)}_{s0\to\phi J/\psi}]/\sqrt{2}$, and $\mathcal{A}_\perp = [\mathcal{A}^{(h=+1)}_{s0\to\phi J/\psi} - \mathcal{A}^{(h=-1)}_{s0\to\phi J/\psi}]/\sqrt{2}$.

The CP average is defined in terms of the polarization fractions, f_k,

$$A_{CP}^k = \frac{f_k^{\bar{B}_s^0} - f_k^{B_s^0}}{f_k^{\bar{B}_s^0} + f_k^{B_s^0}}. \tag{58}$$

Similarly, for $B_s^0 \to f_0(980) J/\psi$, the CP average is defined as,

$$A_{CP} = \frac{\mathcal{B}(\bar{B}_s^0 \to f_0 J/\psi) - \mathcal{B}(B_s^0 \to f_0 J/\psi)}{\mathcal{B}(\bar{B}_s^0 \to f_0 J/\psi) + \mathcal{B}(B_s^0 \to f_0 J/\psi)}. \tag{59}$$

We use data from CDF and DØ for the $B_s^0 \to \phi J/\psi$ decay, whereas there is no available data on the channel $B_s^0 \to f_0 J/\psi$. Our data compilation consists of the DØ values for the amplitudes, $|\mathcal{A}_L|^2 = 0.555 \pm 0.027 \pm 0.006$, $|\mathcal{A}_\parallel|^2 = 0.244 \pm 0.032 \pm 0.014$ and the relative phase $\phi_\parallel = 2.72^{+1.12}_{-0.27}$ rad [7]. The CDF values [33] are compatible, $|\mathcal{A}_L|^2 = 0.530 \pm 0.021 \pm 0.007$ and $|\mathcal{A}_\parallel|^2 = 0.230 \pm 0.027 \pm 0.009$, and the PDG data book quotes the branching fraction, $\mathcal{B}(B_s^0 \to J/\psi\phi) = (9.3 \pm 3.3) \times 10^{-4}$ [18].

The ratio $\mathcal{R}_{f_0/\phi}$ has been argued [8] to be of the order 0.2–0.3, based on the knowledge of the experimental ratio of decay rates [34],

$$\frac{\Gamma(D_s^+ \to f_0\pi^+ \to K^+K^-\pi^-)}{\Gamma(D_s^+ \to \phi\pi^+ \to K^+K^-\pi^-)} = 0.28 \pm 0.12, \tag{60}$$

and an estimate of the semileptonic, integrated branching fraction ratio $\mathcal{B}(D_s^+ \to f_0 e^+\nu, f_0 \to \pi^+\pi^-)/\mathcal{B}(D_s^+ \to \phi e^+\nu, \phi \to K^+K^-) = (13 \pm 4)\%$ from CLEO [35]. The ratio $\mathcal{R}_{f_0/\phi}$ was reassessed in terms of the differential decay ratio [36],

$$\mathcal{R}_{f_0/\phi} = \frac{\frac{d\Gamma}{dq^2}(D_s^+ \to f_0 e^+\nu, f_0 \to \pi^+\pi^-)|_{q^2=0}}{\frac{d\Gamma}{dq^2}(D_s^+ \to \phi e^+\nu, \phi \to K^+K^-)|_{q^2=0}} = 0.42 \pm 0.11. \tag{61}$$

If we combine the above three experimental estimates, we propose a window of $0.2 \lesssim \mathcal{R}_{f_0/\phi} \lesssim 0.5$ for the ratio based on D_s decays.

With the experimental data listed under Eq. (55) as constraint, we find optimal values for X_C and X_H. In principle, we deal with a system of four coupled nonlinear equations for $|\mathcal{A}_L|^2$, $|\mathcal{A}_\parallel|^2$, $\phi_\parallel$ and $\mathcal{B}(B_s^0 \to \phi J/\psi)$ and four variables, which does not put tight constraints on the phenomenological part of our $B_s^0 \to J/\psi\phi$ amplitude. When solving numerically we find, depending on the $f_{B_s^0}$ values, two solutions among which only one yields a reasonable value for the branching fraction $\mathcal{B}(B_s \to f_0 J/\psi)$ not too different from that in a naive quark model. We list the parameters $\rho_{C,H}$ and $\phi_{C,H}$ independent of $\bar{f}_{f_0^s}$ for three values of $f_{B_s^0}$ in Table II, from which it is plain

TABLE II. Values of the higher order correction (ρ_C, ϕ_C) and hard-scattering (ρ_H, ϕ_H) parameters as function of the B_s^0 decay constant.

$f_{B_s^0}$ [MeV]	ρ_C	ϕ_C (°)	ρ_H	ϕ_H (°)
230	4.52 ± 2.24	173.8 ± 37.6	1.90 ± 0.20	266.0 ± 21.6
260	6.16 ± 2.03	176.1 ± 53.6	1.70 ± 0.16	260.6 ± 19.3
290	7.33 ± 1.63	176.0 ± 57.6	1.54 ± 0.15	255.6 ± 17.3

TABLE III. Short-distance amplitudes, $a_n^{q,h}(m_b)\times 10^3$, for the helicity $h=+1$ in $B_s^0\to J/\psi\phi$, as a function of the decay constant, $f_{B_s^0}$, and with $\bar{f}_{f_0^s}=380$ MeV. The $LOVP$ results are obtained with the leading-order (LO) amplitude to which vertex V and penguin P corrections are added. In case of $LOVPH$, the hard-scattering contribution with the end-point parametrization X_H is included. $LOVPH+C$ contains additionally the purely phenomenological contribution $\zeta^{(h)}$ with two more parameters.

$f_{B_s^0}$ [MeV]	230			260		290	
	$LOVP$	$LOVPH$	$LOVPH+C$	$LOVPH$	$LOVPH+C$	$LOVPH$	$LOVPH+C$
$a_2^{u,c}(m_b)$	$60.38-i161.7$	$-3.77+i148.8$	$-8.43+i129.87$	$38.06+i149.7$	$8.21+i130.04$	$75.52+i140.4$	$22.57+i128.49$
$a_3^{u,c}(m_b)$	$5.66+i5.39$	$8.54-i8.54$	$8.75-i7.69$	$6.66-i8.58$	$8.0-i7.70$	$4.98-i8.17$	$7.36-i7.63$
$a_5^{u,c}(m_b)$	$-5.27-i6.28$	$-8.94+i11.47$	$-9.21+i10.39$	$-6.55+i11.52$	$-8.25+i10.40$	$-4.41+i10.99$	$-7.43+i10.31$
$a_7^{u}(m_b)$	$0.12+i0.07$	$0.17-i0.13$	$0.17-i0.12$	$0.14-i0.13$	$0.16-i0.12$	$0.11-i0.13$	$0.15-i0.12$
$a_7^{c}(m_b)$	$0.69+i0.07$	$0.73-i0.13$	$0.74-i0.12$	$0.71-i0.13$	$0.73-i0.12$	$0.68-i0.13$	$0.72-i0.12$
$a_9^{u}(m_b)$	$-9.25-i0.27$	$-9.40+i0.43$	$-9.41+i0.39$	$-9.30+i0.43$	$-9.37+i0.39$	$-9.22+i0.41$	$-9.34+i0.38$
$a_9^{c}(m_b)$	$-8.68-i0.27$	$-8.83+i0.43$	$-8.84+i0.39$	$-8.73+i0.43$	$-8.80+i0.39$	$-8.65+i0.41$	$-8.77+i0.38$

that the uncertainties on the magnitude of the modulus ρ_C as well as the phase ϕ_C are substantial. The experimental errors on the observables are clearly not constraining enough. Yet, we observe that the variations of X_C and X_H are smooth as a function of the decay constant $f_{B_s^0}$.

Likewise, we present numerical values for $a_n^{q,h}(m_b)$ for the three helicities in $B_s^0\to J/\psi\phi$ in Tables III, IV, and V and for $B_s^0\to J/\psi f_0$ in Table VI as functions of $f_{B_s^0}$ to illustrate one facet of the hadronic uncertainty. In these tables, we list the decomposition of $a_n^{q,h}(m_b)$ for each value of $f_{B_s^0}$; in the first column, the values of $a_n^{q,h}(m_b)$ are for the calculated leading-order (LO), vertex (V), and penguin (P) amplitudes only. These are independent of $f_{B_s^0}$ and correspond to the predictions in Fig. 1. Next, the $a_n^{q,h}(m_b)$ that contain the LO, V, P and the hard-scattering (H) amplitudes, where only ρ_H and ϕ_H are fitted to reproduce the $B_s^0\to\phi J/\psi$ observables while $X_C=0$. For $f_{B_s^0}=260$ MeV, one obtains $\rho_H=1.85\pm0.07$ and $\phi_H=255.9\pm24.6$. These values are not very different from those given in the second line of Table II. This case corresponds to Fig. 2. At last, denoted by $LOVPH+C$, we give the values for $a_n^{q,h}(m_b)$ for the case that the $\zeta^{(h)}$ amplitudes are included, which corresponds to the $\rho_{C,H}$ and $\phi_{C,H}$ values in Table II and to Fig. 3. We remind that the dependence on $f_{B_s^0}$ enters the short-distance coefficients via the hard-scattering contribution $H_n^h(M_1J/\psi)$ in Eq. (22) and that the phenomenological amplitudes, X_H and X_C, are in competition with each other. Therefore, the hard-scattering contributions to $a_n^{q,h}(m_b)$ in $LOVPH$ are slightly different than those to $LOVPH+C$.

TABLE IV. Short-distance amplitudes, $a_n^{q,h}(m_b)\times 10^3$, for helicity $h=-1$ and $B_s^0\to J/\psi\phi$. Since the hard-scattering contributions are zero, these amplitudes are independent of $f_{B_s^0}$.

$a_2^{u,c}(m_b)$	-51.72
$a_3^{u,c}(m_b)$	9.39
$a_5^{u,c}(m_b)$	-9.63
$a_7^{u,c}(m_b)$	0.12
$a_9^{u,c}(m_b)$	-9.49

The largest values observed in the leading amplitude, $a_2^{u,c}(m_b)$, are for $h=0$. We also remark there is no variation as a function of f_{B_s} in Table IV since $H_n^{h=-1}(M_1J/\psi)=0$. Moreover, penguin contractions only contribute to $a_7^{q,h=+1}(m_b)$ and $a_9^{q,h=+1}(m_b)$ in the $B_s^0\to\phi J/\psi$ amplitudes, while there are no penguin terms in $B_s^0\to f_0J/\psi$. Altogether, the penguin contributions are very small. We note that the contribution of the phenomenological amplitudes, $\zeta^{(h)}$ (Tables VII and VIII), is small, about 6%–7% of the $h=0,+1$ amplitudes in $B_s\to\phi J/\psi$ and 2% of the $B_s\to f_0J/\psi$ amplitude, yet dominant in the $h=-1$ amplitude devoid of penguin and hard-scattering corrections. Thus, any contribution from new physics, and to less an extent annihilation topologies, should occur in the $h=-1$ helicity amplitude.

When including all the contributions ($LOVPH+C$), we qualitatively verify the hierarchy relation,

TABLE V. As in Table III but for the helicity $h=0$.

$f_{B_s^0}$ [MeV]	230			260		290	
	$LOVP$	$LOVPH$	$LOVPH+C$	$LOVPH$	$LOVPH+C$	$LOVPH$	$LOVPH+C$
$a_2^{u,c}(m_b)$	$54.51-i80.86$	$160.2-i132.6$	$161.0-i129.4$	$165.7-i132.7$	$170.6-i129.5$	$171.8-i131.2$	$180.6-i129.2$
$a_3^{u,c}(m_b)$	$5.86+i2.69$	$1.11+i5.01$	$1.08+i4.87$	$0.87+i5.02$	$0.65+i4.87$	$0.60+i4.95$	$0.20+i4.86$
$a_5^{u,c}(m_b)$	$-7.17-i3.14$	$-1.12-i6.10$	$-1.08-i5.92$	$-0.81-i6.11$	$-0.53-i5.92$	$-0.46-i6.02$	$0.04-i5.90$
$a_7^{u,c}(m_b)$	$0.09+i0.03$	$0.02+i0.07$	$0.02+i0.07$	$0.02+i0.07$	$0.02+i0.07$	$0.02+i0.07$	$0.01+i0.06$
$a_9^{u,c}(m_b)$	$-9.31-i0.14$	$-9.07-i0.25$	$-9.07-i0.24$	$-9.06-i0.25$	$-9.05-i0.24$	$-9.05-i0.25$	$-9.03-i0.24$

TABLE VI. Short-distance amplitudes, $a_n^q(m_b) \times 10^3$, for $B_s^0 \to J/\psi f_0(980)$ as a function of the $f_{B_s^0}$ decay constant with $\bar{f}_{f_0^s} = 380$ MeV and $F_1^{B_s^0 \to f_0^s}(m_{J/\psi}^2) = 0.4$. See caption in Table III for the definition of *LOVP*, *LOVPH*, and *LOVPH* + *C* amplitudes.

$f_{B_s^0}$ [MeV]	230			260		290	
	LOVP	*LOVPH*	*LOVPH* + *C*	*LOVPH*	*LOVPH* + *C*	*LOVPH*	*LOVPH* + *C*
$a_2^{u,c}(m_b)$	$11.61 - i80.86$	$-42.40 - i255.5$	$-33.35 - i224.3$	$-66.51 - i234.1$	$-51.82 - i224.4$	$-95.23 - i229.5$	$-69.17 - i223.8$
$a_3^{u,c}(m_b)$	$7.29 + i2.69$	$9.71 + i10.53$	$9.30 + i9.13$	$10.80 + i9.57$	$10.13 + i9.13$	$12.08 + i9.36$	$10.91 + i9.10$
$a_5^{u,c}(m_b)$	$-7.17 - i3.14$	$-10.25 - i13.12$	$-9.74 - i11.34$	$-11.63 - i11.90$	$-10.79 - i11.35$	$-13.27 - i11.64$	$-11.78 - i11.31$
$a_7^{u,c}(m_b)$	$0.09 + 0.03$	$0.13 + i0.15$	$0.12 + i0.13$	$0.14 + i0.14$	$0.14 + i0.13$	$0.16 + i0.13$	$0.15 + i0.13$
$a_9^{u,c}(m_b)$	$-9.38 - i0.14$	$-9.51 - i0.53$	$-9.49 - i0.46$	$-9.56 - i0.48$	$-9.53 - i0.46$	$-9.63 - i0.47$	$-9.57 - i0.46$

$|\mathcal{A}^{(h=0)}_{B_s^0 \to \phi J/\psi}| > |\mathcal{A}^{(h=+1)}_{B_s^0 \to \phi J/\psi}| > |\mathcal{A}^{(h=-1)}_{B_s^0 \to \phi J/\psi}|$, in $B_s^0 \to J/\psi\phi$ and $|\mathcal{A}^{(h=0)}_{B_s^0 \to \phi J/\psi}| > |\mathcal{A}^{(h=-1)}_{B_s^0 \to \phi J/\psi}| > |\mathcal{A}^{(h=+1)}_{B_s^0 \to \phi J/\psi}|$ in the *CP* conjugate decay $\bar{B}_s^0 \to J/\psi\phi$. These hierarchy relations are also reproduced for the amplitudes when they include, besides tree contributions, vertex, penguin and hard-scattering corrections.

Having determined numerical values for X_H and X_C, we can calculate the $B_s^0 \to f_0 J/\psi$ amplitude and obtain the associated branching fraction and *CP* asymmetry. We do so for the central values of $f_{B_s^0} = 260$ MeV and $\bar{f}_{f_0^s} = 380$ MeV discussed in Sec. V. For a transition form factor $F_1^{B_s^0 \to f_0^s}(q^2 = m_{J/\psi}^2) = 0.4$ and for the different amplitudes *LOVP*, *LOVPH*, and *LOVPH* + *C* defined above, those observables are displayed in Table IX together with a comparison of the $B_s^0 \to J/\psi\phi$ results with the corresponding available experimental analysis values. Furthermore, we obtain for a transition form factor $F_1^{B_s^0 \to f_0^s}(q^2 = m_{J/\psi}^2) = 0.2$:

$$\mathcal{B}(B_s \to f_0 J/\psi) = 3.80 \times 10^{-4},$$
$$A_{CP}(B_s \to f_0 J/\psi) = -0.0005,$$
$$\mathcal{B}(B_s \to \phi J/\psi) = 9.30 \times 10^{-4},$$
$$\mathcal{R}_{f_0/\phi} = 0.42;$$

for $F_1^{B_s^0 \to f_0^s}(q^2 = m_{J/\psi}^2) = 0.3$,

$$\mathcal{B}(B_s \to f_0 J/\psi) = 4.37 \times 10^{-4},$$
$$A_{CP}(B_s \to f_0 J/\psi) = -0.0008,$$
$$\mathcal{B}(B_s \to \phi J/\psi) = 9.30 \times 10^{-4},$$
$$\mathcal{R}_{f_0/\phi} = 0.48;$$

and for $F_1^{B_s^0 \to f_0^s}(q^2 = m_{J/\psi}^2) = 0.5$,

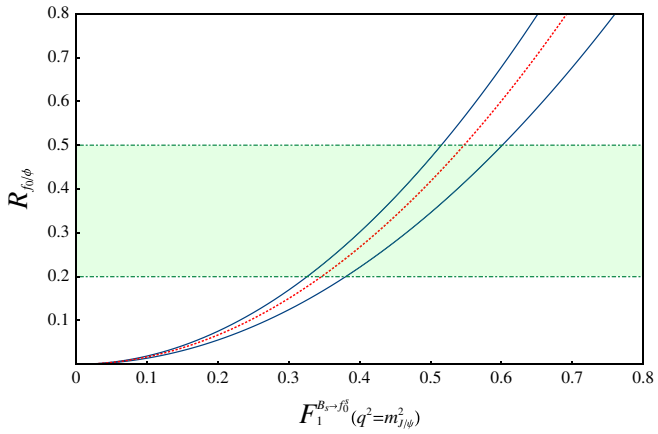

FIG. 1 (color online). The ratio $\mathcal{R}_{f_0/\phi}$ as a function of the transition form factor $F_1^{B_s^0 \to f_0^s}(m_{J/\psi}^2)$. Only tree, vertex, and penguin contributions (*LOVP*), independent of the decay constants $f_{B_s^0}$ and $\bar{f}_{f_0}$, are included in the decay amplitudes. The dotted line corresponds to the central value of this ratio while the area between the two solid lines gives its envelope due to the uncertainties on the decay rates $f_0(980) \to \pi^+\pi^-$ [10,36] and $\phi \to K^+K^-$ [18]. The two horizontal dash-dotted lines delimit the (shaded) area between the experimental predictions found in Refs. [8,36].

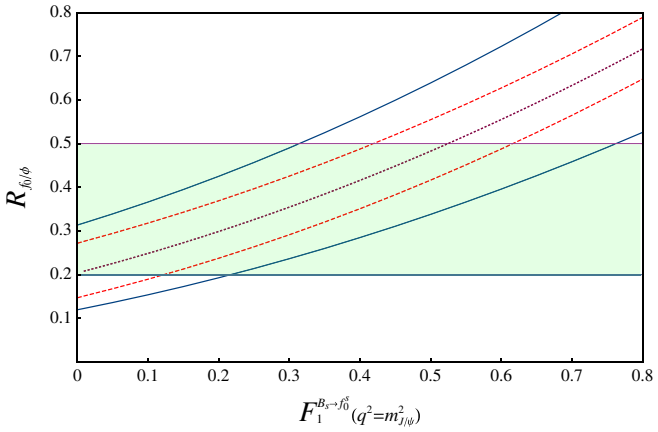

FIG. 2 (color online). The ratio $\mathcal{R}_{f_0/\phi}$ as a function of the transition form factor $F_1^{B_s^0 \to f_0^s}(m_{J/\psi}^2)$ where now the tree, vertex, penguin, and hard-scattering contributions (*LOVPH*) are included. The area between the two dashed lines gives the envelope of this ratio when taking into account uncertainties on the decay constants ($f_{B_s^0} = 260 \pm 30$ MeV and $\bar{f}_{f_0} = 380 \pm 40$ MeV) while the solid lines include in addition the uncertainties on the decay rates $f_0(980) \to \pi^+\pi^-$ [10,36] and $\phi \to K^+K^-$ [18]. The single dotted line is our prediction for the central values of the decay constants, $f_{B_s^0} = 260$ MeV and $\bar{f}_{f_0} = 380$ MeV. The horizontal dash-dotted lines correspond to the experimental predictions of Refs. [8,36].

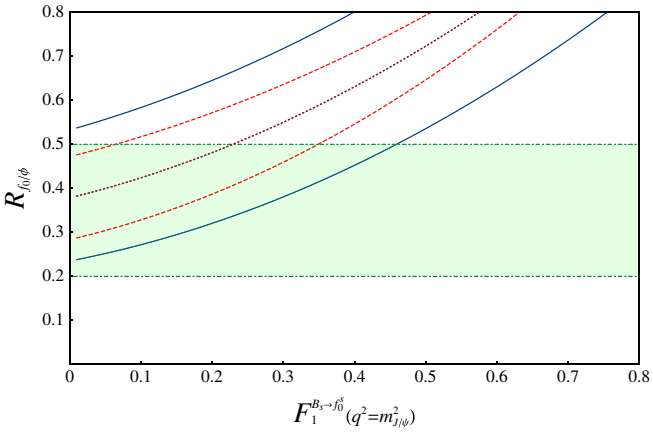

FIG. 3 (color online). Same as in Fig. 2 but including $\zeta^{(h)}$ contributions ($LOVPH + C$ amplitudes).

$$\mathcal{B}(B_s \to f_0 J/\psi) = 5.7 \times 10^{-4},$$
$$A_{CP}(B_s \to f_0 J/\psi) = -0.0013,$$
$$\mathcal{B}(B_s \to \phi J/\psi) = 9.30 \times 10^{-4},$$
$$\mathcal{R}_{f_0/\phi} = 0.63,$$

and finally, the CP asymmetries in $B_s \to J/\psi\phi$ are

$$A_{CP}^{L}(B_s \to \phi J/\psi) = -1.66 \times 10^{-3},$$
$$A_{CP}^{\parallel}(B_s \to \phi J/\psi) = 1.99 \times 10^{-3},$$
$$A_{CP}^{\perp}(B_s \to \phi J/\psi) = 2.15 \times 10^{-3}.$$

Our prediction for the time-integrated asymmetry $A_{CP}(B_s \to f_0 J/\psi)$ is about 1 order of magnitude smaller than the standard model value, $-2\beta_s = -0.036$. We remark that the above numerical values for this CP asymmetry have to be interpreted with care—we choose the parameters of the full QCDF amplitude in Table II such that the experimental $B_s^0 \to J/\psi\phi$ observables are reproduced. In doing so, we may deliberately include "new physics" effects with just the standard model amplitude, in particular, via the additional amplitudes $\zeta^{(h)}$. Moreover, we use the same end point parametrization, X_H, in both decay channels since the $B_s^0 \to J/\psi f_0$ branching ratio is not experimentally known. This approach seems reasonable, as the physics buried in these infrared divergences must be similar in both decays. It could also lead to an overestimation of the hard-scattering contributions to $B_s^0 \to J/\psi f_0$ as well as of $A_{CP}(B_s \to f_0 J/\psi)$.

We illustrate the variation of the ratio, $\mathcal{R}_{f_0/\phi}$, by taking into account the uncertainties in the decay constants $f_{B_s^0}$ and $\bar{f}_{f_0^s}$ as well as those in the decay rates, $\mathcal{B}(f_0(980) \to \pi^+\pi^-) = 0.50^{+0.07}_{-0.09}$ [10,36] and $\mathcal{B}(\phi \to K^+K^-) = 0.489 \pm 0.005$ [18]. The results are displayed in Figs. 1–3.

In Fig. 1, $\mathcal{R}_{f_0/\phi}$ is plotted as a function of $F_1^{B_s^0\to f_0^s}(m_{J/\psi}^2)$ where only the tree amplitude along with vertex and penguin corrections are included in both amplitudes, $\mathcal{A}^h_{B_s^0\to\phi J/\psi}$ and $\mathcal{A}_{B_s^0\to f_0 J/\psi}$. The ratio is plotted with the corresponding envelope of $\mathcal{R}_{f_0/\phi}$ due to the uncertainty on the decay rates. In Fig. 2, we augment this amplitude by hard-scattering contributions, that is the full QCDF amplitude given in Eq. (22). Finally, in Fig. 3, $\mathcal{R}_{f_0/\phi}$ is plotted as a function of $F_1^{B_s^0\to f_0^s}(m_{J/\psi}^2)$ including hard-scattering corrections and possible other contributions, $\zeta^{(h)}$. Although the aforementioned uncertainties are depicted in all figures,

TABLE VII. The phenomenological contributions $\zeta^h \times 10^3$ for $h = 0, -1, +1$, Eq. (22), to the $B_s^0 \to J/\psi\phi$ amplitude as a function of the $f_{B_s^0}$ decay constant with $\bar{f}_{f_0^s} = 380$ MeV.

$f_{B_s^0}$ [MeV]	230	260	290
$\zeta^{h=0}$	$-18.11 + i1.98$	$-28.04 + i1.89$	$-37.19 + i2.63$
$\zeta^{h=-1}$	$-129.26 + i14.12$	$-200.12 + i13.46$	$-265.41 + i18.77$
$\zeta^{h=+1}$	$-15.25 + i1.67$	$-23.61 + i1.59$	$-31.31 + i2.21$

TABLE VIII. Same as Table VII but for the $B_s^0 \to J/\psi f_0(980)$ amplitude.

$f_{B_s^0}$ [MeV]	230	260	290
ζ	$-44.08 + i4.81$	$-68.25 + i4.59$	$-90.51 + i6.40$

TABLE IX. Prediction for the $B_s^0 \to J/\psi f_0$ observables for the different amplitudes $LOVP$, $LOVPH$, and $LOVPH + C$ along with experimental analysis data of the $B_s^0 \to J/\psi\phi$ decay. Here central values, $f_{B_s^0} = 260$ MeV and $\bar{f}_{f_0^s} = 380$ MeV and the transition form factor $F_1^{B_s^0\to f_0^s}(q^2 = m_{J/\psi}^2) = 0.4$ are used. The values in the second column are predictions. Those of the third column include the hard-scattering corrections with the end-point parametrization $\rho_H = 1.85 \pm 0.07$ and $\phi_H = 255.9° \pm 24.6°$. The fourth column corresponds to the reproduction of the data with the parameters ρ_H, ϕ_H, ρ_C, and ϕ_C displayed in the second line of Table II.

	$LOVP$ (Prediction)	$LOVPH$ (2 parameters)	$LOVPH + C$ (4 parameters)	Experimental data
$\lvert\mathcal{A}_L\rvert^2$	0.172	0.554	0.555	0.555 ± 0.033 [7]
$\lvert\mathcal{A}_\parallel\rvert^2$	0.404	0.219	0.244	0.244 ± 0.046 [7]
$\phi_\parallel$(rad)	−0.221	2.13	2.72	2.72 ± 1.38 [7]
$\mathcal{B}(B_s^0 \to J/\psi\phi)$	0.00075	0.00115	0.00093	0.00093 ± 0.00033 [18]
$\mathcal{B}(B_s^0 \to J/\psi f_0)$	0.00020	0.00047	0.00050	
$A_{CP}(B_s^0 \to J/\psi f_0)$	−0.00013	−0.0013	−0.0011	
$\mathcal{R}_{f_0/\phi}$	0.28	0.42	0.55	

we stress that those on the decay constants $f_{B_s^0}$ and $\bar{f}_{f_0^s}$, where they apply, have more impact on the $\mathcal{R}_{f_0/\phi}$ band than the $f_0(980)$ and ϕ decay rate incertitudes. The spreading of the curves representing $\mathcal{R}_{f_0/\phi}$ as a function of $F_1^{B_s^0\to f_0^s}(m_{J/\psi}^2)$ is larger with respect to the variation in $f_{B_s^0}$ than in $\bar{f}_{f_0^s}$. This points to the necessity of having an improved experimental determination of $f_{B_s^0}$. The upper limit of the envelope is reached only for the largest values of $f_{B_s^0}$ and $\bar{f}_{f_0^s}$ considered here.

Figure 3 shows that our central-value predictions of $\mathcal{R}_{f_0/\phi}$, in absence of any phenomenological contributions, are within the estimate by Stone and Zhang [8] for most values of the form factor $F_1^{B_s^0\to f_0^s}(m_{J/\psi}^2)$. However, when the additional amplitudes, ζ, are accounted for in the decay amplitudes of Eqs. (2) and (4), the ratio $\mathcal{R}_{f_0/\phi}$ exhibits three striking features:

(i) Additional amplitudes, ζ, can play a major role due to their large contributions to both the numerator and denominator of the ratio $\mathcal{R}_{f_0/\phi}$, as seen from the comparison of Figs. 2 and 3.

(ii) The predicted $\mathcal{R}_{f_0/\phi}$ band overlaps well with the estimates of Refs. [8,36] for $F_1^{B_s^0\to f_0^s}(m_{J/\psi}^2) < 0.4$; beyond, our predictions are much larger, which may indicate a larger pollution due to $f_0(980) \to K^+K^-$ if contributions from other than the standard model were present.

(iii) The uncertainties on the $f_0(980)$ and ϕ decay rates increase the width of the band considerably, though the main uncertainty stems from the decay constants $f_{B_s^0}$ and $\bar{f}_{f_0}$.

Let us recall that the decay constant $\bar{f}_{f_0^s}$ only enters the hard-scattering and additional phenomenological contributions (C) to the decay amplitude $B_s^0 \to f_0(980)J/\psi$. If these are turned off, as in Fig. 1, the ratio $R_{f_0/\phi}$ is still significantly above 10% for realistic transition form factor values. That said, for practical purposes we decide to only consider the more recently obtained decay constants in Ref. [22] and choose three values within the given errors, $\bar{f}_{f_0^s} = 340, 380, 420$ MeV. The value 180 MeV [25] yields too low branching fractions in other decays, for example $B \to f_0(980)\pi, f_0(980)\rho, f_0(980)K^{(*)}$. Nevertheless, since we fix the hard-scattering parameters, ρ_H and ϕ_H, only via the decay $B_s^0 \to J/\psi\phi$ and $\bar{f}_{f_0^s}$ enters the numerator in $\mathcal{R}_{f_0/\phi}$ linearly, the modification is straightforward: $\bar{f}_{f_0^s} = 180$ MeV is about half the value $\bar{f}_{f_0^s} = 380$ MeV, therefore the central value of $\mathcal{R}_{f_0\phi}$ in Fig. 2 decreases from 0.42 to 0.19 (for $F_0^{B_s^0\to f_0^s} = 0.4$). This is still within the limits predicted by the experimental estimates, $0.2 \lesssim \mathcal{R}_{f_0/\phi} \lesssim 0.5$, and implies an S-wave pollution.

We infer from our numerical results that S-wave kaons or pions under the ϕ peak in $B_s^0 \to J/\psi\phi$ are very likely to originate from the similar decay $B_s^0 \to J/\psi f_0$. Therefore, the extraction of the mixing phase, $-2\beta_s$, from $B_s^0 \to J/\psi\phi$ may well be biased by this S-wave effect which should be taken into account in experimental analyses. In our interpretation of the full QCDF amplitude, we not only confirm the influence of S-wave contamination as advocated in Refs. [8,36] but also find that its effect could be sizable.

VII. CONCLUSIVE OUTLOOK

The "phase" of $B_s^0 - \bar{B}_s^0$ mixing, $-2\beta_s$, is thought to be best measured in the golden decay, $B_s^0 \to J/\psi\phi$, and provides an opportune place to investigate physics beyond the standard model. Several models have been proposed to explain the apparent discrepancy of the standard model prediction for $-2\beta_s$ with recent experiments, in particular, exploring the impact of heavy, as of yet undiscovered particles on CP violation in weak B-meson decays. A general analysis of possible new physics effects in the case of $B_s^0 - \bar{B}_s^0$ mixing was recently given by Chiang *et al.* [21]. In there, the authors investigate several beyond standard model variations of the $B_s \to J/\psi\phi$ decay, such as $Z^{(\prime)}$-mediated flavor changing neutral currents, two Higgs doublets and SUSY, and find that new physics contributions may only modestly contribute to the mixing phase. However, it is also concluded, somewhat prematurely, that the CDF and DØ results are clear signs of new physics.

In the present paper, we have taken a different path and studied the contamination of final-state S-waves kaons in the $B_s^0 \to J/\psi\phi$ channel by those originating from the $f_0(980)$ in the very similar $B_s^0 \to J/\psi f_0(980)$ decay. We find that this effect is strong enough already for amplitudes including leading-order, vertex, and penguin corrections to create a real bias in the determination of $-2\beta_s$.

Of course, we are aware that the phenomenological endpoint parametrization of α_s corrections in the amplitudes $H_n(M_1J/\psi)$ and $H_n^h(M_1J/\psi)$ can cloud possible new physics contributions alongside the $\zeta^{(h)}$ contributions. In this case, we suppose that any new effects should be of comparable magnitude in $B_s^0 \to J/\psi\phi$ and $B_s^0 \to J/\psi f_0(980)$. Therefore, the S-wave contamination would be on the upper side of the estimate we propound and future analyses of the mixing angle in B_s decays should be concerned with this effect.

ACKNOWLEDGMENTS

The authors are obliged to Sheldon Stone for pointing out the likely S-wave effects on the mixing angle which stimulated this work and critical remarks on the manuscript. We thank Martin Beneke for useful comments on mass corrections in transition form factors between two mesons. We are very grateful to Ying Li for drawing our attention to the particular quark topology of the annihilation diagrams.

B. E. wishes to acknowledge the hospitality of the *Laboratoire de Physique Nucléaire et Hautes Energies* in Paris and of João Pacheco, B. C. de Melo, and Victo dos Santos Filho at Universidade Cruzeiro do Sul, São Paulo, during the final stage of the writing. This work was partially funded by the Department of Energy, Office of Nuclear Physics, under Contract No. DE-AC02-06CH11357.

[1] O. Leitner, J. P. Dedonder, B. Loiseau, and R. Kaminski, Phys. Rev. D **81**, 094033 (2010).
[2] B. El-Bennich, A. Furman, R. Kamiński, L. Leśniak, and B. Loiseau, Phys. Rev. D **74**, 114009 (2006).
[3] D. R. Boito, J.-P. Dedonder, B. El-Bennich, O. Leitner, and B. Loiseau, Phys. Rev. D **79**, 034020 (2009).
[4] B. El-Bennich, A. Furman, R. Kamiński, L. Leśniak, B. Loiseau, and B. Moussallam, Phys. Rev. D **79**, 094005 (2009).
[5] T. Aaltonen *et al.* (CDF Collaboration), Phys. Rev. Lett. **100**, 161802 (2008).
[6] V. M. Abazov *et al.* (DØ Collaboration), Phys. Rev. Lett. **101**, 241801 (2008).
[7] V. M. Abazov *et al.* (DØ Collaboration), Phys. Rev. Lett. **102**, 032001 (2009).
[8] S. Stone and L. Zhang, Phys. Rev. D **79**, 074024 (2009); arXiv:0909.5442.
[9] Y. Xie, P. Clarke, G. Cowan, and F. Muheim, J. High Energy Phys. 09 (2009) 074.
[10] B. El-Bennich, O. Leitner, J.-P. Dedonder, and B. Loiseau, Phys. Rev. D **79**, 076004 (2009).
[11] M. Beneke, G. Buchalla, M. Neubert, and C. T. Sachrajda, Nucl. Phys. **B591**, 313 (2000).
[12] M. Beneke, G. Buchalla, M. Neubert, and C. T. Sachrajda, Nucl. Phys. **B606**, 245 (2001).
[13] M. Beneke and M. Neubert, Nucl. Phys. **B675**, 333 (2003).
[14] M. Beneke, J. Rohrer, and D. Yang, Nucl. Phys. **B774**, 64 (2007).
[15] J. Chay and C. Kim, arXiv:hep-ph/0009244.
[16] H. Y. Cheng, Y. Y. Keum, and K. C. Yang, Phys. Rev. D **65**, 094023 (2002).
[17] M. Beneke and L. Vernazza, Nucl. Phys. **B811**, 155 (2009).
[18] C. Amsler *et al.* (Particle Data Group), Phys. Lett. B **667**, 1 (2008).
[19] D. Melikhov, Eur. Phys. J. direct C **4**, 1 (2002).
[20] X. Q. Li, G. R. Lu, and Y. D. Yang, Phys. Rev. D **68**, 114015 (2003); **71**, 019902(E) (2005).
[21] C. W. Chiang, A. Datta, M. Duraisamy, D. London, M. Nagashima, and A. Szynkman, J. High Energy Phys. 04 (2010) 31.
[22] H. Y. Cheng, C. K. Chua, and K. C. Yang, Phys. Rev. D **73**, 014017 (2006).
[23] M. Beneke, J. Rohrer, and D. Yang, Phys. Rev. Lett. **96**, 141801 (2006).
[24] C. W. Hwang and Z. T. Wei, J. Phys. G **34**, 687 (2007).
[25] F. De Fazio and M. R. Pennington, Phys. Lett. B **521**, 15 (2001).
[26] L. Lellouch and C. J. D. Lin (UKQCD Collaboration), Phys. Rev. D **64**, 094501 (2001).
[27] A. Gray *et al.* (HPQCD Collaboration), Phys. Rev. Lett. **95**, 212001 (2005).
[28] E. Gámiz, C. T. H. Davies, G. P. Lepage, J. Shigemitsu, and M. Wingate (HPQCD Collaboration), Phys. Rev. D **80**, 014503 (2009).
[29] N. Ghahramany and R. Khosravi, Phys. Rev. D **80**, 016009 (2009).
[30] P. Colangelo, F. De Fazio and W. Wang, Phys. Rev. D **81**, 074001 (2010).
[31] R. H. Li, C. D. Lu, W. Wang, and X. X. Wang, Phys. Rev. D **79**, 014013 (2009).
[32] B. El-Bennich, M. A. Ivanov, and C. D. Roberts, Nucl. Phys. B, Proc. Suppl. **199**, 184 (2010).
[33] T. Kuhr (CDF Collaboration), arXiv:0710.1789.
[34] P. L. Frabetti *et al.* (E687 Collaboration), Phys. Lett. B **351**, 591 (1995).
[35] J. Yelton *et al.* (CLEO Collaboration), Phys. Rev. D **80**, 052007 (2009).
[36] K. M. Ecklund *et al.* (CLEO Collaboration), Phys. Rev. D **80**, 052009 (2009).